

Role of Ptc2 Type 2C Ser/Thr Phosphatase in Yeast High-Osmolarity Glycerol Pathway Inactivation

Christian Young, James Mapes, Jennifer Hanneman, Sheikha Al-Zarban, and Irene Ota*

Department of Chemistry and Biochemistry, University of Colorado, Boulder, Colorado 80309-0215

Received 15 May 2002/Accepted 10 September 2002

Three type 2C Ser/Thr phosphatases (PTCs) are negative regulators of the yeast *Saccharomyces cerevisiae* high-osmolarity glycerol mitogen-activated protein kinase (MAPK) pathway. Ptc2 and Ptc3 are 75% identical to each other and differ from Ptc1 in having a noncatalytic domain. Previously, we showed that Ptc1 inactivates the pathway by dephosphorylating the Hog1 MAPK; Ptc1 maintains low basal Hog1 activity and dephosphorylates Hog1 during adaptation. Here, we examined the function of Ptc2 and Ptc3. First, deletion of *PTC2* and/or *PTC3* together with *PTP2*, encoding the protein tyrosine phosphatase that inactivates Hog1, produced a strong growth defect at 37°C that was dependent on *HOG1*, providing further evidence that *PTC2* and *PTC3* are negative regulators. Second, overexpression of *PTC2* inhibited Hog1 activation but did not affect Hog1-Tyr phosphorylation, suggesting that Ptc2 inactivates the pathway by dephosphorylating the Hog1 activation loop phosphothreonine (pThr) residue. Indeed, in vitro studies confirmed that Ptc2 was specific for Hog1-pThr. Third, deletion of both *PTC2* and *PTC3* led to greater Hog1 activation upon osmotic stress than was observed in wild-type strains, although no obvious change in Hog1 inactivation during adaptation was seen. These results indicate that Ptc2 and Ptc3 differ from Ptc1 in that they limit maximal Hog1 activity. The function of the Ptc2 noncatalytic domain was also examined. Deletion of this domain decreased V_{max} by 1.6-fold and increased K_m by 2-fold. Thus Ptc2 requires an additional amino acid sequence beyond the catalytic domain defined for PTCs for full activity.

The yeast *Saccharomyces cerevisiae* high-osmolarity glycerol (HOG) mitogen-activated protein kinase (MAPK) pathway regulates the response to osmotic stress (8) and is also activated by heat stress (38). Like other MAPK pathways, the HOG pathway contains a three-kinase module: a MEKK (MAPK/ERK kinase kinase) which phosphorylates a MEK (MAPK/ERK kinase), which in turn phosphorylates a MAPK (8, 25). Activated MEKK phosphorylates MEK at conserved Ser and Thr residues, resulting in MEK activation. Activated MEK phosphorylates the conserved Thr-X-Tyr motif in the activation loop of MAPK, where X is Glu, Pro, or Gly. In the HOG pathway, three MEKKs, Ssk2, Ssk22, and Ste11, activate the MEK Pbs2 and the MAPK Hog1 (8). The HOG pathway contains two upstream branches that converge at Pbs2. One branch is the two-component signaling system containing Sln1, Ypd1, and Ssk1, which negatively regulates the downstream MAPK cascade (15, 28). The second branch contains the membrane-bound Sho1 (13), which positively regulates the MAPK cascade via Cdc42, Ste20, Ste50, and Ste11 (23, 26, 27, 29, 30).

Critical to the proper regulation of MAPK pathways is their inactivation. For example, mutations that block the inactivation of these pathways are detrimental for development and cell growth. In *Drosophila melanogaster*, inactivation of *puckered*, which encodes a dual-specificity phosphatase that regulates c-Jun N-terminal kinase, results in defects in dorsal closure during embryogenesis (17, 41). In the *S. cerevisiae* HOG pathway, deletion of the negative regulator *SLN1* is lethal (24) due to hyperactivation of Hog1 (15). Furthermore, deletion of

PTP2, encoding a protein tyrosine phosphatase (PTP) that dephosphorylates Hog1, and *PTC1*, coding for a type 2C Ser/Thr phosphatase (PP2C or PTC in yeast) that dephosphorylates Hog1, produces a severe growth defect due to hyperactivation of Hog1 (12, 14).

Two groups of protein phosphatases inactivate the HOG pathway. The PTPs Ptp2 and Ptp3 inactivate the Hog1 MAPK by dephosphorylating the phosphotyrosine residue in the activation loop (12, 40). Ptp2 plays the major role in inactivating Hog1 in vivo. For example, a strain lacking *PTP2* more poorly dephosphorylates Hog1-phosphotyrosine (Hog1-pY) than a strain lacking *PTP3*. However, Ptp3 is important for Hog1 inactivation, as deletion of both *PTP2* and *PTP3* results in a severe defect in Hog1-pY dephosphorylation (12, 40). The differences in the activities of Ptp2 and Ptp3 may be explained by their relative abilities to bind Hog1, as well as their differential subcellular localizations. Ptp2 binds Hog1 more effectively than Ptp3 (12), and Ptp2 is nuclear whereas Ptp3 is cytoplasmic (19). Since Hog1 accumulates in the nucleus upon activation (5, 18, 31), the nuclear localization of Ptp2 might contribute to its greater activity. A second group of phosphatases, the PTCs, have been identified as negative regulators of the HOG pathway and of MAPK pathways in vertebrates and in plants (9, 10, 20, 35). These phosphatases differ from other Ser/Thr phosphatases in being monomeric enzymes that require Mg^{2+} or Mn^{2+} for catalytic activity (1, 36). Three genes, *PTC1*, *PTC2*, and *PTC3*, encode PTCs which have been linked to the HOG pathway. They are multicopy suppressors of *sln1Δ* lethality, which is due to hyperactivation of the downstream MAPK cascade (15, 37). We showed that the catalytic activity of each of the PTCs was important for HOG pathway inactivation, as mutation of conserved Asp residues that constitute

* Corresponding author. Mailing address: Myriad Proteomics, 2150 W. Dauntless Ave., Salt Lake City, UT 84116. Phone: (801) 303-1799. Fax: (801) 303-1701. E-mail: ota@myriad-proteomics.com.

TABLE 1. Yeast strains

Strain	Genotype	Reference or source
Strain BBY45 and strains derived from it		
BBY45	<i>MATa trp1-1 ura3-52 his3-Δ200 leu2-3,112 lys2-801 gal</i>	2
IMY21a	<i>MATa ptp2Δ::HIS3 trp1-1 ura3-52 his3-Δ200 leu2-3,112 lys2-801 gal</i>	24
IMY124	<i>MATa ptc2Δ::TRP1 ptc3Δ::HIS3 trp1-1 ura3-52 his3-Δ200 leu2-3,112 lys2-801 gal</i>	37
IMY126	<i>MATa ptc2Δ::TRP1 ptp2Δ::HIS3 trp1-1 ura3-52 his3-Δ200 leu2-3,112 lys2-801 gal</i>	37
IMY127b	<i>MATα ptc3Δ::HIS3 ptp2Δ::HIS3 trp1-1 ura3-52 his3-Δ200 leu2-3,112 lys2-801 gal</i>	37
IMY128	<i>MATα ptc2Δ::TRP1 ptc3Δ::HIS3 ptp2Δ::HIS3 trp1-1 ura3-52 his3-Δ200 leu2-3,112 lys2-801 gal</i>	37
ACB4	<i>MATα hog1Δ::kanMX trp1-1 ura3-52 his3-Δ200 leu2-3,112 lys2-801 gal</i>	This work
ACB5	<i>MATa ptc2Δ::TRP1 ptp2Δ::HIS3 hog1Δ::kanMX trp1-1 ura3-52 his3-Δ200 leu2-3,112 lys2-801 gal</i>	This work
JMY1	<i>MATα ptc3Δ::HIS3 ptp2Δ::HIS3 hog1Δ::kanMX trp1-1 ura3-52 his3-Δ200 leu2-3,112 lys2-801 gal</i>	This work
JMY2	<i>MATα ptc2Δ::TRP1 ptc3Δ::HIS3 ptp2Δ::HIS3 hog1Δ::kanMX trp1-1 ura3-52 his3-Δ200 leu2-3,112 lys2-801 gal</i>	This work
IMY100	<i>MATa hog1Δ::TRP1 trp1-1 ura3-52 his3-Δ200 leu2-3,112 lys2-801 gal</i>	12
IMY120b	<i>MATα ptc2Δ::TRP1 trp1-1 ura3-52 his3-Δ200 leu2-3,112 lys2-801 gal</i>	37
CYY1	<i>MATa ptc2Δ::TRP1 hog1Δ::TRP1 trp1-1 ura3-52 his3-Δ200 leu2-3,112 lys2-801 gal</i>	This work
IMY121b	<i>MATα ptc3Δ::HIS3 trp1-1 ura3-52 his3-Δ200 leu2-3,112 lys2-801 gal</i>	37
CYY2	<i>MATa ptc3Δ::HIS3 hog1Δ::TRP1 trp1-1 ura3-52 his3-Δ200 leu2-3,112 lys2-801 gal</i>	This work
CAY9	<i>MATa ptc2Δ::TRP1 ptc3Δ::HIS3 hog1Δ::TRP1 trp1-1 ura3-52 his3-Δ200 leu2-3,112 lys2-801 gal</i>	This work
IMY101	<i>MATa sln1Δ::HIS3 trp1-1 ura3-52 his3-Δ200 leu2-3,112 lys2-801 gal</i>	12
Strain 334 and a strain derived from it		
334	<i>MATα leu2-3,112 gal1 reg1-501 ura3-52 pep4-3 prb1-1122</i>	11
IMY105	<i>MATα hog1::hisG leu2-3,112 gal1 reg1-501 ura3-52 pep4-3 prb1-1122</i>	37

the metal binding site prevented them from suppressing the *sln1Δ* lethal phenotype (37). Ptc2 and Ptc3 differ from Ptc1 in that they contain carboxy-terminal noncatalytic domains of ~170 residues not found in Ptc1. A fourth PTC, Ptc4, most closely related in primary structure to Ptc1, Ptc2, and Ptc3, was not able to suppress *sln1Δ* lethality (37), suggesting that *PTC1*, *PTC2*, and *PTC3* are the most important genes for HOG pathway inactivation.

Previously, we showed that Ptc1 inactivates the HOG pathway by acting on Hog1 (37). *PTC1* overexpression blocked osmotic-stress-induced Hog1 activation. In contrast, deletion of *PTC1* elevated Hog1 basal activity and inhibited Hog1 inactivation during adaptation. Ptc1 performed these functions by specifically dephosphorylating the Hog1-phosphothreonine residue in the activation loop. Ptc1 did not have a strong effect on the Pbs2 MEK in vivo (37), although vertebrate PTCs could inactivate stress-activated MEKs and MEKs (9, 35).

In this work we examined the function of the Ptc2 and Ptc3 phosphatases. Ptc2 and Ptc3 may have similar functions, as they are 75% identical to each other. We believed that their functions might be different from those of Ptc1, as Ptc2 and Ptc3 contain an additional noncatalytic domain. Ptc2 and Ptc3 were similar to Ptc1 in that they inactivated Hog1. However, unlike deletion of *PTC1*, deletion of *PTC2* and *PTC3* did not alter basal Hog1 activity or adaptation but rather resulted in hyperactivation of Hog1 upon osmotic stress. Therefore, Ptc2 and Ptc3 limit maximal Hog1 activation, while Ptc1 regulates Hog1 basal activity and its dephosphorylation during adaptation. In this way, the three PTCs acting on this pathway have complementary roles in regulating Hog1.

MATERIALS AND METHODS

Yeast strains, media, and genetic techniques. The yeast strains used in this work are described in Table 1. The temperature sensitivity of strains lacking *PTCs* and *PTP2* was assessed in the BBY45 background (2). ACB5 (*MATa*

ptc2Δ::TRP1 ptp2Δ::HIS3 hog1Δ::kanMX) was produced by crossing IMY126 (*MATa ptc2Δ::TRP1 ptp2Δ::HIS3*) (37) with ACB4 (*MATα hog1Δ::kanMX*). JMY1 (*MATα ptc3Δ::HIS3 ptp2Δ::HIS3 hog1Δ::kanMX*) and JMY2 (*MATα ptc2Δ::TRP1 ptc3Δ::HIS3 ptp2Δ::HIS3 hog1Δ::kanMX*) were produced by transforming IMY127b (37) and IMY128 (37), respectively, with the *hog1Δ::kanMX* allele. The *hog1Δ* allele was produced by PCR using oligonucleotides complementary to *HOG1* and *kanMX* contained in the plasmid pRS400 (3). Media to culture yeast were produced essentially as described by Sherman et al. (33). Hog1 kinase assays were performed with the following strains. IMY105 (*MATα hog1::hisG*) (37), derived from 334 (11), overexpressed *PTC2* from pKT-PTC2 (see below) and expressed Hog1 fused to the hemagglutinin (HA) epitope (Hog1-HA) from the pHOG1-ha2 plasmid (37). Hog1 kinase assays of *ptcΔ* strains were performed in the BBY45 background (2). CYY1 (*MATa ptc2Δ::TRP1 hog1Δ::TRP1*) was produced by mating IMY120b (*MATα ptc2Δ::TRP1*) (2) to IMY100 (*MATa hog1Δ::TRP1*) (12) carrying pHOG1-ha2. CYY2 (*MATa ptc3Δ::HIS3 hog1Δ::TRP1*) was produced by mating IMY121b (*MATα ptc3Δ::HIS3*) (37) to IMY100 carrying pHOG1-ha2. Tetrads were dissected to isolate the desired strains. CAY9 (*MATa ptc2Δ::TRP1 ptc3Δ::HIS3 hog1Δ::TRP1*) originated from a cross between IMY100b (*MATα hog1Δ::TRP1*) (12) and IMY124 (*MATa ptc2Δ::TRP1 ptc3Δ::HIS3*) (37). CAY9 was transformed with pHOG1-ha3 (2 μ m *LEU2*), which expressed the same endogenous promoter-driven Hog1-HA as pHOG1-ha2 (2 μ m *HIS3*) (37), but from YE-plac181 (2 μ m *LEU2*) (7).

The ability of Ptc2 mutant proteins lacking portions of the noncatalytic domain to inactivate the HOG pathway was examined by a phenotypic assay that we described previously (12). Deletion of *SLN1* is lethal due to hyperactivation of the downstream HOG MAPK cascade (15). Increased expression of protein phosphatases that inactivate the MAPK cascade allows the *sln1Δ* strain to survive (12, 37). Plasmids carrying *PTC2* and truncated *PTC2* mutants were transformed into IMY101, a *sln1Δ::HIS3* strain containing the plasmid pSLN1-URA3, a low-copy-number, *CEN*-based plasmid carrying the wild-type *SLN1* gene and the *URA3* gene (12). Growth of the strain on 5-fluoroorotic acid (5-FOA)-containing media occurs when the pSLN1-URA3 plasmid is lost, indicating that the phosphatase is active.

Plasmids. The 6xHis-Ptc2 protein was produced in *Escherichia coli* by using the pRSETA-PTC2 plasmid. A *Bam*HI site was introduced directly upstream of the start codon with the oligonucleotides 5'-GCGGATCCATGGACAAATTC TATCAAAC-3', containing the restriction site (underlined), and 5'-CGGAAT TCTCACAGCGCGACAACCACTATACTC-3'. The resulting fragment, containing the 5' end of *PTC2*, was digested with *Bam*HI and *Clal*I (an endogenous site) and ligated together with the 3' end of *PTC2* contained in an 800-bp *Clal*-*Pst*I fragment into pRSETA (Invitrogen) to produce pRSETA-PTC2.

Ptc2 truncation mutant proteins Ptc2 (1-312), Ptc2 (1-355), and Ptc2 (1-412) were expressed in yeast and in *E. coli*. PCR was performed with a common 5' primer containing a *Bam*HI site (underlined), 5'-GCGGGATCCAATGATGGCAAATACGC-3', and one of three 3' primers, either 5'-GCAAGCTTTAGCGTGGGGCCTTGGACTTCATAC-3', 5'-GCAAGCTTTAGTGGTCGCGAGTGAATTGTCC-3', or 5'-GCAAGCTTTATCTGTAGCACCAAGTAGCGCC-3' (*Hind*III sites are underlined and stop codons are italicized), which were used to produce Ptc2 (1-312), Ptc2 (1-355), and Ptc2 (1-412), respectively. For expression in yeast, the PCR products were digested with *Bam*HI and *Hind*III and ligated into the multicopy vector YEplac181 (7) to produce the plasmids pPTC2 (1-312), pPTC2 (1-355), and pPTC2 (1-412). The Ptc2 truncation mutants were also expressed in *E. coli* by using the pRSETA vector. The plasmids pPTC2 (1-312), pPTC2 (1-355), and pPTC2 (1-412) were digested with *Cla*I and *Hind*III to isolate the 3' end of the gene and cloned into pRSETA-PTC2 digested with the same enzymes.

Glutathione *S*-transferase (GST) or green fluorescent protein (GFP) was fused to Ptc2 and Ptc3, and the fusion proteins were expressed in yeast from the following plasmids. The pKT-PTC2 plasmid was used to overexpress GST-Ptc2. *PTC2* was isolated from pRSETA-PTC2 and cloned into p(EG)KT (21). Ptc2 and Ptc3 localization was examined by fusing GFP to their carboxy-terminal ends. PCR was used to replace the *PTC2* and *PTC3* stop codons with *Not*I sites, and a *Not*I fragment containing the GFP coding sequence (a gift from J. Hirsch, Columbia University) was inserted. The Ptc2-GFP fusion protein was expressed from its endogenous promoter in pRS426 (2 μ m *URA3*) and pRS316 (*CEN URA3*). Ptc3-GFP was expressed from its endogenous promoter in pRS424 (2 μ m *TRP1*) and in pRS314 (*CEN TRP1*) (34). Both the Ptc2-GFP and Ptc3-GFP fusion proteins were functional, as they suppressed *sln1* Δ lethality due to HOG pathway hyperactivation, as judged by the 5-FOA test described above (12). For the *sln1* Δ suppression assay, Ptc2-GFP was subcloned into the plasmid pRS424 (2 μ m *TRP1*) and Ptc3-GFP was expressed from the same pRS424 plasmid described above.

Expression and purification of Ptc2 and Ptc2 truncation mutant proteins from *E. coli*. 6xHis-Ptc2 and 6xHis-Ptc2 truncation mutants were expressed in *E. coli* and purified by metal affinity chromatography; the methods used were similar to those described by Warmka et al. (37). The plasmids pRSETA-Ptc2, pRSETA-Ptc2 (1-312), pRSETA-Ptc2 (1-355), and pRSETA-Ptc2 (1-412) were transformed into *E. coli* strain BL21(DE3)pLysS (Novagen), and expression was induced with 0.4 mM isopropyl- β -D-thiogalactopyranoside for 3 h at 23°C. The 6xHis-Ptc2 proteins were purified with Co²⁺-immobilized metal affinity resin (TALON; Clontech) and eluted with elution buffer I (20 mM Tris-HCl [pH 8.0], 100 mM NaCl, 75 mM imidazole). Fractions containing 6xHis-Ptc2 proteins were identified by immunoblotting with an anti-His₆ antibody (Babco). The isolated 6xHis-Ptc2 proteins were greater than 99% pure as judged by Coomassie staining and were quantified by using the bicinchoninic acid protein assay (Pierce).

Ptc2 inactivation of Hog1 kinase in vitro. Ptc2 inactivation of Hog1 was performed essentially as described previously (37). 6xHis-Ptc2 purified from *E. coli* was incubated with osmotic-stress-activated GST-Hog1 isolated from yeast strain IMY105 carrying pKT-HOG1 (37). GST-Hog1 activity was assessed by examining its ability to phosphorylate myelin basic protein (MBP; Sigma). Buffers A and C, used to isolate GST-Hog1 (37), were modified so that each contained 5 mM MnCl₂ instead of 5 mM MgCl₂. Phosphatase assay buffer (37) was modified to contain 20 mM MnCl₂ instead of 5 mM MgCl₂. GST-Hog1 bound to glutathione-Sepharose (Pharmacia) was aliquoted into fractions containing ~0.5 μ g of GST-Hog1 and dephosphorylated with 0 to 1.2 μ g of 6xHis-Ptc2 for 30 min at 37°C. GST-Hog1 was incubated with 1 μ M MBP and 0.1 mM [γ -³²P]ATP (8,000 cpm/pmol) for 30 min at 30°C to examine the remaining kinase activity (37). Incorporation of ³²P into MBP was examined by sodium dodecyl sulfate-polyacrylamide gel electrophoresis and PhosphorImager analysis (Molecular Dynamics).

Phosphoamino acid analysis. ³²P-labeled Hog1 was untreated or was incubated with 6xHis-Ptc2, and phosphoamino acid analysis was performed as described previously (37). Briefly, GST-Hog1, isolated from yeast strain IMY105, carrying pKT-HOG1 (37), was phosphorylated in vitro with hyperactive MEK mutant Pbs2EE and [γ -³²P]ATP. Approximately 2.5 μ g of ³²P-GST-Hog1 bound to glutathione-Sepharose was incubated with 1.5 μ g of 6xHis-Ptc2 for 30 min at 37°C. GST-Hog1 was isolated by sodium dodecyl sulfate-polyacrylamide gel electrophoresis and transferred to polyvinylidene difluoride. GST-Hog1 was excised from the membrane and subjected to acid hydrolysis, and phosphoamino acid analysis was performed.

Ptc2 inactivation of Hog1 in vivo. Hog1 kinase activity was assayed according to the methods described by Warmka et al. (37). Strains overexpressing *PTC2* or deleted for PTCs and expressing Hog1-HA as described above were grown in selective media to an *A*₆₀₀ of 1 and were untreated or exposed to 0.4 M NaCl for

various times. Cells were disrupted in buffer A with glass beads, and Hog1-HA was immunoprecipitated with an anti-HA antibody (HA.11; Covance) and protein G-agarose (Santa Cruz Biotechnology) (37). Hog1 kinase activity was assayed by using 1 μ M MBP (Sigma) and 0.1 mM [γ -³²P]ATP (8,000 cpm/pmol) and by incubating cells for 30 min at 30°C.

Immunoblotting. Endogenous Hog1 Tyr phosphorylation in the yeast strain 334 (11), overexpressing *PTC2* from the plasmid pKT-PTC2 described above or carrying empty vector pEG(KT), was examined (21). Cells in exponential growth phase were untreated or exposed to 0.4 M NaCl for various times, and samples were prepared for immunoblotting as described previously (12). Protein in cell lysates was quantified by the bicinchoninic acid protein assay (Pierce), and Hog1 Tyr phosphorylation was monitored by immunoblotting with an antiphosphotyrosine antibody (PY99; Santa Cruz Biotechnology). GST-Ptc2 and GST were detected with an anti-GST antibody (Pharmacia), and Hog1 was visualized with an anti-Hog1 antibody (yC-20; Santa Cruz Biotechnology).

Assay for phosphatase activity using pNPP. The activity of 6xHis-Ptc2 and 6xHis-Ptc2 truncation proteins was assessed by using *p*-nitrophenyl phosphate (*p*NPP) as the substrate. Seven-picomole samples of 6xHis-Ptc2, 6xHis-Ptc2 (1-312), 6xHis-Ptc2 (1-355), and 6xHis-Ptc2 (1-412) contained in 100 μ l of elution buffer I were incubated at 30°C with 100 μ l of phosphatase buffer (100 mM imidazole [pH 7.5], 10 mM dithiothreitol, 10 mM MnCl₂) containing 400 μ M to 200 mM *p*NPP. Hydrolysis of *p*NPP was monitored by recording changes in absorbance at 405 nm over time and was linear from 0 to 100 min of incubation. The change in *A*₄₀₅ versus time was plotted by using Kaleidagraph software, and best-fit-line equations were generated to determine velocity.

Fluorescence microscopy. The subcellular localization of Ptc2-GFP and Ptc3-GFP in the *ptc2* Δ strain IMY120b (37) and the *ptc3* Δ strain IMY121b (37), respectively, was examined. Cultures in exponential growth phase were untreated or exposed to 0.4 M NaCl at 30°C for various times before examining PTC-GFP localization. DAPI (4',6'-diamidino-2-phenylindole) was used to visualize the nucleus. Images were captured with a Zeiss Axioplan fluorescence microscope with a Sensys digital charge-coupled device camera system and processed by using IP-LAB Spectrum software.

RESULTS

Strains lacking *PTC2*, *PTC3*, and *PTP2* have a temperature-sensitive defect due to *HOG1*. The *sln1* Δ lethal phenotype, which is due to HOG pathway hyperactivation, is suppressed by *PTC2* and *PTC3* expression from multicopy plasmids (15, 37). Here we tested whether the phenotype of *PTC* deletion mutants would also show a connection to the HOG pathway. Previously, we reported that strains lacking *PTC2* and/or *PTC3* and *PTP2*, encoding the PTP that inactivates Hog1, exhibited temperature-sensitive defects (27). Briefly, the *ptc3* Δ *ptp2* Δ and *ptc2* Δ *ptp2* Δ (data not shown) double mutants grew more poorly than the wild type at 37°C but grew normally at 30°C (Fig. 1A). Furthermore, the *ptc2* Δ *ptc3* Δ *ptp2* Δ triple mutant grew slightly worse than the *ptc2* Δ *ptp2* Δ and *ptc3* Δ *ptp2* Δ double mutants at 37°C but showed no obvious defect at 30°C (Fig. 1A). We tested whether these temperature-sensitive defects could be due to *HOG1*. This seemed possible, since we recently found that the HOG pathway is activated by heat stress and that a strain lacking the PTPs that inactivate Hog1 is lethal at 37°C due to Hog1 hyperactivation (38). To test this possibility, *HOG1* was deleted in the phosphatase-null backgrounds. The *ptc2* Δ *ptc3* Δ *ptp2* Δ *hog1* Δ strain grew significantly better than the *ptc2* Δ *ptc3* Δ *ptp2* Δ strain at 37°C (Fig. 1B). In addition, *ptc3* Δ *ptp2* Δ *hog1* Δ (Fig. 1B) and *ptc2* Δ *ptp2* Δ *hog1* Δ (data not shown) strains each showed improved growth at 37°C, relative to *ptc3* Δ *ptp2* Δ (Fig. 1A) and *ptc2* Δ *ptp2* Δ strains. Therefore, strains lacking *PTCs* and *PTP2* exhibit temperature sensitivity which is dependent on *HOG1*.

Ptc2 inactivates Hog1 in vitro by dephosphorylating phos-

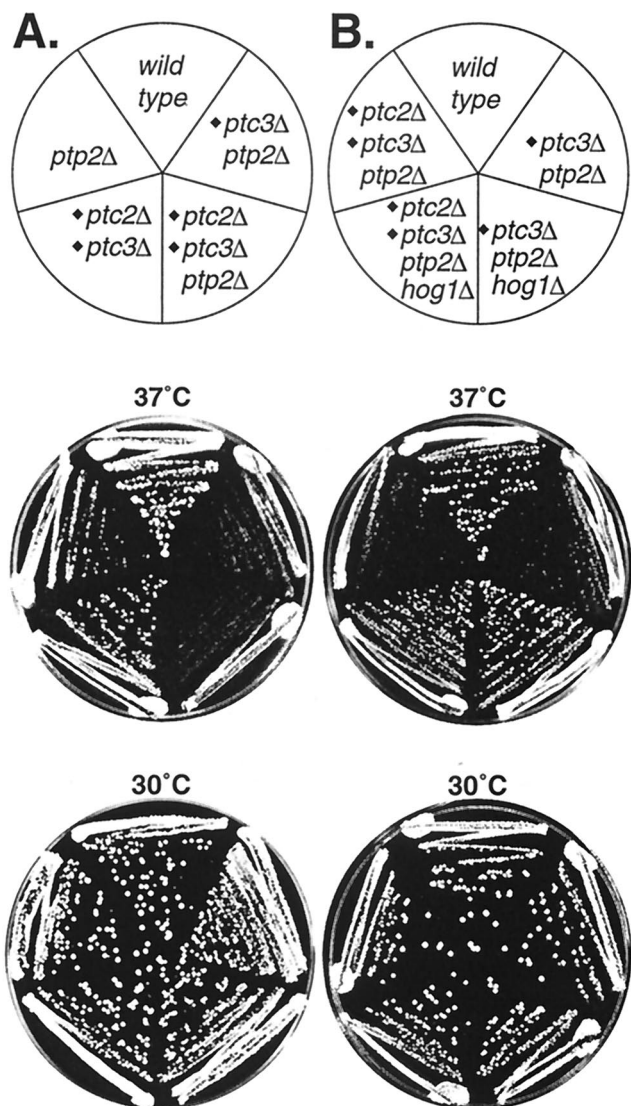


FIG. 1. The temperature sensitivity of strains lacking *PTCs* and *PTP2* is due to *HOG1*. (A) Strains lacking *PTCs* and *PTP2* exhibit growth defects at 37°C. The growth of *ptp2Δ* (IMY21a), *ptc2Δ ptc3Δ* (IMY124), *ptc3Δ ptp2Δ* (IMY127b), *ptc2Δ ptc3Δ ptp2Δ* (IMY128), and wild-type (BBY45) strains on rich medium (yeast extract-peptone-dextrose [YPD]) at 37 and 30°C was compared. (B) The growth defects of the *ptc3Δ ptp2Δ* and *ptc2Δ ptc3Δ ptp2Δ* strains at 37°C were suppressed by deleting *HOG1*. The strains lacking *HOG1* were JMY1 (*ptc3Δ ptp2Δ hog1Δ*) and JMY2 (*ptc2Δ ptc3Δ ptp2Δ hog1Δ*) and were compared on YPD at 37 and 30°C.

phosphothreonine. Previously, we showed that Ptc1 inactivates the HOG pathway by dephosphorylating Hog1. Since Ptc2 belongs to the same class of PTC phosphatases, we asked whether Ptc2 could also inactivate Hog1. We first tested whether Ptc2 could inactivate Hog1 in vitro. Activated Hog1 was isolated from osmotic stressed yeast and treated with Ptc2, which was expressed in *E. coli* and purified by affinity chromatography. Hog1 kinase activity was examined by using MBP and [γ - 32 P]ATP as substrates. Ptc2 readily inactivated Hog1 (Fig. 2A), similar to Ptc1 (37).

To examine the mechanism by which Ptc2 inactivates Hog1,

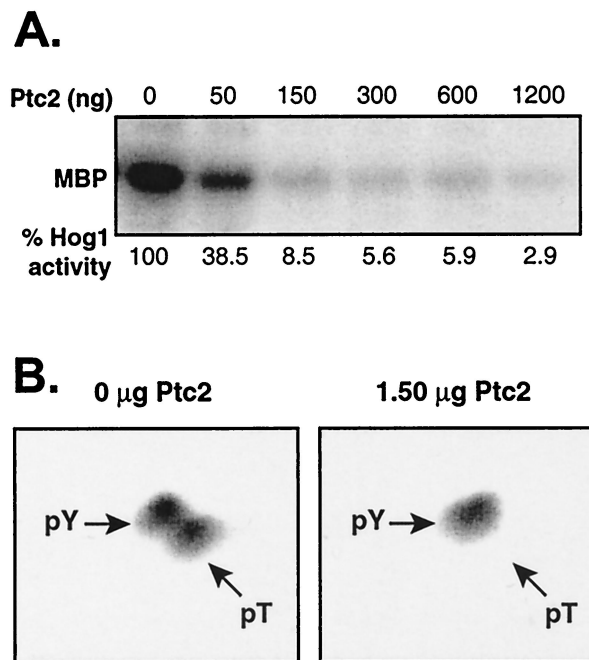


FIG. 2. Ptc2 inactivates Hog1 in vitro. (A) Activated GST-Hog1 was isolated from osmotic stressed yeast and was untreated or treated with Ptc2. Approximately 0.5 μ g of GST-Hog1 bound to resin was incubated with 0 to 1.2 μ g of Ptc2 for 30 min at 30°C. The resin was washed extensively to remove Ptc2, and GST-Hog1 was incubated with MBP and [γ - 32 P]ATP to assess Hog1 kinase activity. Radiolabel incorporated into MBP was examined by PhosphorImager analysis. (B) Ptc2 inactivates Hog1 by dephosphorylating the phosphothreonine residue (pT) in the activation loop. GST-Hog1 was phosphorylated in vitro, and the sample was untreated (left) or incubated with Ptc2 (right) prior to phosphoamino acid analysis. The radiolabeled amino acids were detected with the PhosphorImager. Arrows, positions of phosphoamino acid standards as revealed by ninhydrin staining.

we asked whether Ptc2 dephosphorylated the Hog1 activation loop Thr or Tyr residue. Since phosphorylation at both sites is required for full activity, Ptc2 could inactivate Hog1 by dephosphorylating either or both residues. Phosphorylated Hog1 was prepared in vitro by using the hyperactive MEK Pbs2EE (37) and [γ - 32 P]ATP. Prior to treatment with Ptc2, Hog1 was phosphorylated nearly equally at Thr and Tyr residues (Fig. 2B), which are in the activation loop (37). Following treatment with Ptc2, the [32 P]phosphothreonine signal was eliminated while the [32 P]phosphotyrosine residue was unchanged (Fig. 2B). Thus, Ptc2 inactivates Hog1 by specifically dephosphorylating the activation loop phosphothreonine residue.

Ptc2 inactivates Hog1 in vivo. Since Ptc2 inactivated Hog1 in vitro, we tested whether it could also inactivate Hog1 in vivo. Hog1 activity was examined in untreated and osmotic stressed cells exposed to 0.4 M NaCl in a strain overexpressing *PTC2* and in a control strain carrying empty vector. Overexpression of *PTC2* inhibited maximal activity approximately threefold (Fig. 3A). In the *PTC2* overexpressor, Hog1 activity increased fourfold upon osmotic stress, whereas in the wild type it increased sevenfold (Fig. 3A). The level of Hog1 protein was the same in the two strains, suggesting that the decrease in activity in the overexpressor was due to a change in phosphorylation.

Since overexpression of *PTC2* inhibited Hog1 activation, we

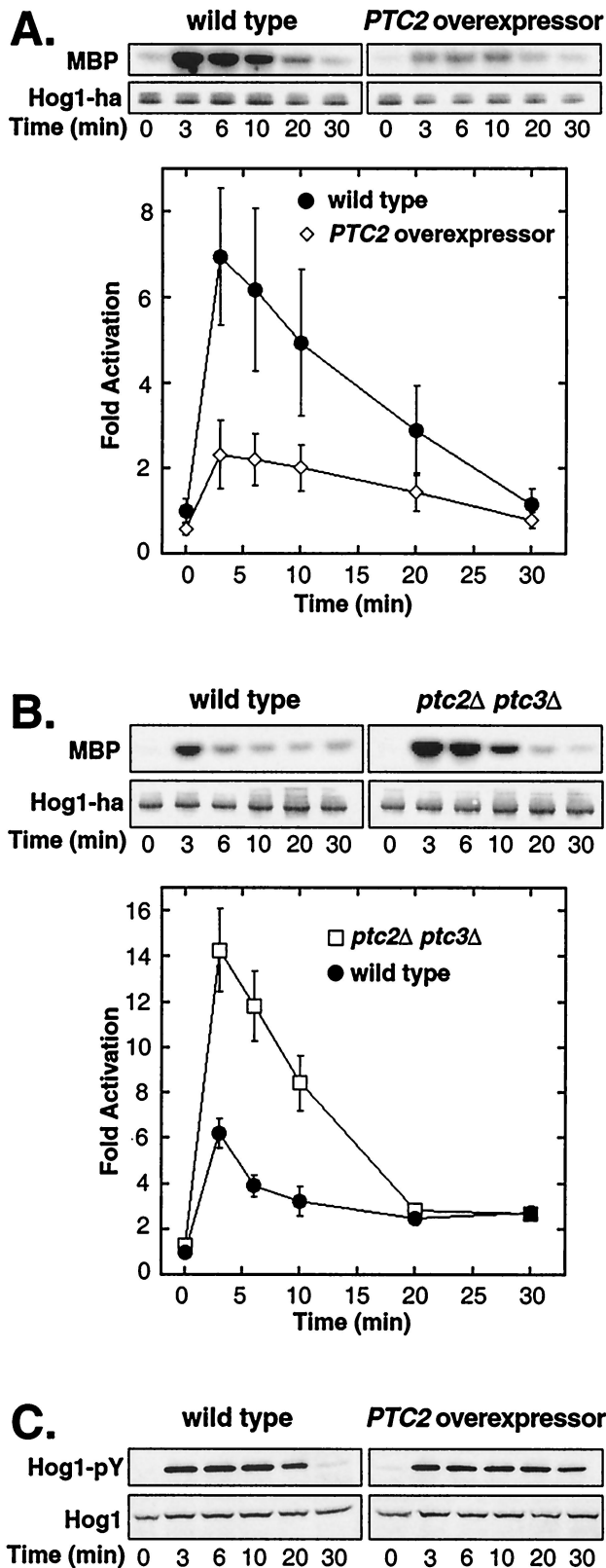


FIG. 3. Ptc2 inactivates Hog1 in vivo. (A) Overexpression of *PTC2* inhibits osmotic-stress-induced Hog1 activation. Hog1 kinase activity in *PTC2* overexpressor IMY105, carrying pKT-*PTC2* and pHOG1-ha2, and in the control strain, carrying empty vector pKT and pHOG1-ha2,

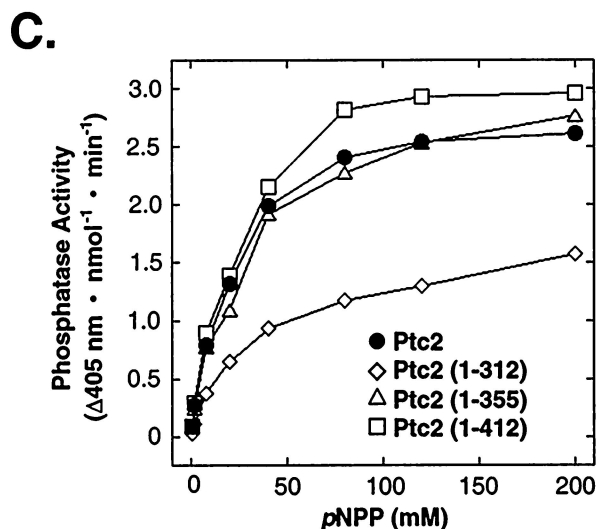
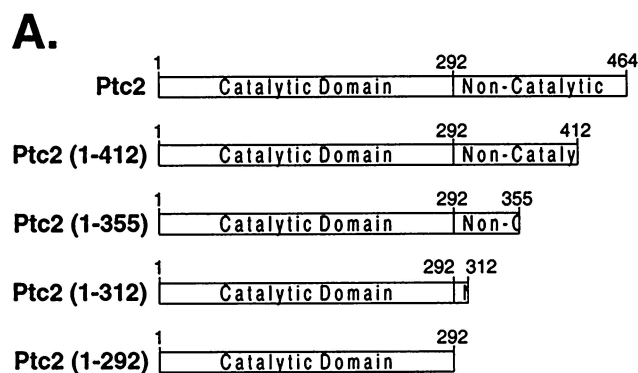
tested whether its deletion might elevate Hog1 activity. However, the *ptc2Δ* strain showed a level of Hog1 activity similar to that for the wild type (data not shown). Since Ptc2 is 75% identical to Ptc3, the effect of deleting *PTC2* might be obscured by *PTC3*. Therefore, we also examined Hog1 activation in *ptc3Δ* and *ptc2Δ ptc3Δ* strains. Deletion of *PTC3* alone had little effect on Hog1 activation (data not shown). However, deletion of both *PTC2* and *PTC3* had a significant effect. In the *ptc2Δ ptc3Δ* strain, Hog1 activity increased 11-fold upon osmotic stress, whereas it increased 6-fold in the wild type (Fig. 3B). The elevated Hog1 activity in the *ptc2Δ ptc3Δ* strain was likely due to phosphorylation, as the level of Hog1 protein in the mutant was comparable to that in the wild type (Fig. 3B). These results indicate that Ptc2 and Ptc3 have redundant functions in this pathway and that they set a maximum level to which Hog1 can be activated.

The results above suggested that Ptc2 acted on Hog1 in vivo; however, they did not exclude the possibility that Ptc2 could act upstream of Hog1. For example, since the MEK Pbs2 requires phosphorylation on Ser and Thr residues for activity (13), its dephosphorylation would also affect Hog1 activity. If Ptc2 inactivates Pbs2, then overexpressing *PTC2* should inhibit Hog1 phosphorylation. We monitored Hog1 Tyr phosphorylation (Hog1-pY), since its Thr phosphorylation would be affected by Ptc2, as shown above (Fig. 2B). Overexpression of *PTC2* did not strongly affect the level of Hog1-pY induced by osmotic stress (Fig. 3C), suggesting that Ptc2 has little effect on Pbs2 or activators upstream of Pbs2.

A portion of the Ptc2 noncatalytic domain is needed for activity. Ptc2 and Ptc3 differ from Ptc1 in that they each have a carboxy-terminal noncatalytic domain of ~170 residues. To examine the function of this domain, a series of deletion mutants was produced (Fig. 4A) and their ability to suppress the *sln1Δ* lethal phenotype due to Hog1 hyperactivation was assessed. The truncation mutant proteins Ptc2 (1-312) (Fig. 4B) and Ptc2 (1-292) (data not shown) were unable to suppress *sln1Δ* lethality. Since Ptc2 (1-292) was very poorly expressed in yeast (data not shown), it was not studied further. Ptc2 (1-355) and Ptc2 (1-412) suppressed *sln1Δ* lethality similarly to full-length Ptc2 (Fig. 4B). In some cases, they appeared to suppress better than the wild type (data not shown).

To investigate why the Ptc2 truncation mutants showed differences in the phenotypic assay relative to the full-length protein, their phosphatase activity was examined in vitro. Ptc2

was examined. Before (time zero) and after exposure to osmotic stress (0.4 M NaCl) for various times, Hog1-HA was immunoprecipitated and incubated with MBP and [γ - 32 P]ATP. Radiolabel incorporated into MBP was examined with the PhosphorImager. The graph shows the means of three independent experiments \pm standard errors of the means (SEM). (B) Hog1 is hyperactivated in a strain lacking *PTC2* and *PTC3*. Hog1 kinase activity was monitored prior to and following osmotic stress in a *hog1Δ* strain (IMY100) and in a *ptc2Δ ptc3Δ hog1Δ* strain (CAY9), each carrying a Hog1-HA-expressing plasmid. Hog1 kinase activity was monitored as described for panel A. The graph shows the means of six independent experiments \pm SEM. (C) Ptc2 does not inactivate Pbs2 in vivo. Hog1-pY in the 334 strain carrying a plasmid overexpressing *PTC2* or an empty vector was examined. The level of Hog1-pY prior to and following osmotic stress was monitored by immunoblotting with an anti-pY antibody. Total Hog1 protein was examined by blotting with an anti-Hog1 antibody.



and the Ptc2 truncation proteins were expressed as His₆ fusions in *E. coli* and purified by Co²⁺ affinity chromatography. With pNPP as a substrate, Ptc2 (1-312) had a 1.6-fold lower V_{max} and 2-fold-higher K_m than full-length Ptc2 (1-464) (Fig. 4C), while the corresponding values for Ptc2 (1-355) and Ptc2 (1-412) were similar to those for the wild type. Therefore, the inability of Ptc2 (1-312) to inactivate the HOG pathway, as judged by the *sln1Δ* lethality suppression test (Fig. 4B), can be explained by its decreased catalytic activity. Thus, the catalytic domain, defined by similarity to other PTC sequences, is not sufficient for full Ptc2 activity.

Ptc2 and Ptc3 subcellular localization. The subcellular localization of MAPK phosphatases is important to consider, as MAPKs including Hog1 accumulate in the nucleus upon activation and redistribute to the cytoplasm during adaptation (5, 18, 31). Therefore, protein phosphatases that regulate maximal Hog1 activity might be expected to be nuclear. The subcellular localization of Ptc2 and Ptc3 was examined by producing functional fusions to GFP. Both Ptc2-GFP and Ptc3-GFP were evenly distributed between the cytoplasm and the nucleus when expressed from low-copy-number or multicopy plasmids in their respective null backgrounds (Fig. 5). Therefore, Ptc2 and Ptc3 could control maximal Hog1 activity. PTC-GFP lo-

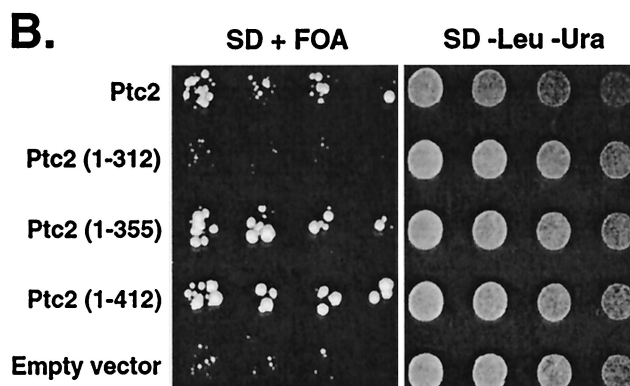


FIG. 4. Analysis of Ptc2 noncatalytic domain function. (A) Schematic representation of Ptc2 and Ptc2 truncation mutant proteins. Full-length Ptc2 is 464 residues with an ~292-residue catalytic domain and an ~172-residue noncatalytic domain. The catalytic domain was assigned by comparison to *S. cerevisiae* Ptc1 (32) and human PP2C α (16). (B) The truncation mutant Ptc2 (1-312) cannot inactivate the HOG pathway. The ability of the Ptc2 truncation proteins to suppress *sln1Δ* lethality was assayed as described in Materials and Methods. The *sln1Δ* strain carrying pSLN1-URA3 was transformed with a plasmid expressing full-length Ptc2, the plasmids expressing the truncation mutant proteins Ptc2 (1-312), Ptc2 (1-355), and Ptc2 (1-412), or an empty vector. The transformants were grown in 8 ml of synthetic medium lacking uracil and leucine to an A_{600} of 1. The cells were concentrated by centrifugation and resuspended in 0.5 ml of water. Twofold serial dilutions were spotted onto synthetic media containing 5-FOA (SD + FOA) or a control lacking FOA and grown at 30°C. Wild-type and mutant Ptc2 proteins were expressed at similar levels as judged by examination of corresponding HA-tagged proteins (not shown). (C) A portion of the noncatalytic domain of Ptc2 is required for full phosphatase activity. Ptc2 and Ptc2 truncation mutants Ptc2 (1-312), Ptc2 (1-355), and Ptc2 (1-412) were purified from *E. coli* as His₆ fusion proteins and incubated with pNPP at the indicated concentrations. Rates were determined by measuring the production of p-nitrophenol at 405 nm and are expressed as the change in absorbance at 405 nm per nanomole of phosphatase per minute.

calization upon osmotic stress was also examined. However, no change in localization was observed with Ptc2-GFP or Ptc3-GFP (data not shown).

DISCUSSION

Hog1 MAPK activity is under coordinate regulation by the PTCs Ptc2 and Ptc3 and the PTPs Ptp2 and Ptp3. The PTCs regulate the level of Hog1 activation loop Thr phosphorylation (Fig. 2) (37), while the PTPs regulate the level of Tyr phosphorylation (12, 39). The focus of this study was the Ptc2 and Ptc3 phosphatases, which are 75% identical to each other, being related by a genome duplication event (39), and which show functional similarity in this pathway (37; this work). First, Ptc2 inactivated Hog1 activity in vitro (Fig. 2A) and specifically dephosphorylated the phosphothreonine residue, which is needed for activity (Fig. 2B). Second, Ptc2 inactivated Hog1 in vivo. Its overexpression inhibited Hog1 activation upon osmotic stress (Fig. 3A), and Ptc2 acted together with Ptc3 to inactivate Hog1. Whereas deletion of *PTC2* or *PTC3* had no effect on Hog1 activity, the *ptc2Δ ptc3Δ* double mutant showed Hog1 hyperactivation in osmotic stressed cells (Fig. 3B). Taken together, these results indicate that Ptc2 and Ptc3 inactivate

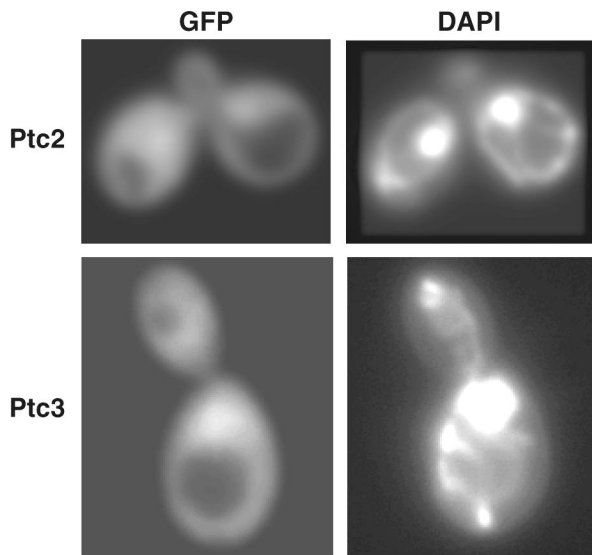


FIG. 5. Ptc2 and Ptc3 are localized to the cytoplasm and nucleus. Ptc2-GFP and Ptc3-GFP were expressed from low-copy-number *CEN*-based plasmids in *ptc2Δ* and *ptc3Δ* strains, respectively. The PTC-GFP fusion proteins were visualized by fluorescence microscopy, and DAPI was used to identify the nucleus.

the HOG pathway by dephosphorylating Hog1-phosphothreonine.

Our results also showed that Ptc2 had little effect on components of the pathway upstream of Hog1. For example, *PTC2* overexpression did not significantly reduce Hog1 Tyr phosphorylation (Fig. 3C), suggesting that it had little effect on Pbs2 or upstream components of the HOG pathway. However, we cannot unequivocally state that Ptc2 has no activity on Pbs2, as we were not able to measure Pbs2 activity directly. An unexpected effect of *PTC2* overexpression was that Hog1-pY could be detected after 30 min of osmotic stress (Fig. 3C), whereas little Hog1-pY was seen in the wild type. Similar results were obtained with *PTC1* overexpression (37). Hog1 Tyr phosphorylation may be prolonged in these *PTC* overexpressors because they might block the access of Ptp2 and Ptp3 to Hog1. Like *S. cerevisiae*, the *Schizosaccharomyces pombe* PTCs that regulate a stress-activated MAPK pathway have little effect on upstream regulators of MAPK (6, 22). The vertebrate PTCs differ from those of the yeasts in that they appear to act on MEKs, MEKs, and p38, a stress-activated MAPK (9, 10, 35). How these differences in specificity between the yeast and vertebrate PTCs arise is not known, but they are likely to be due to different sequence elements within PTCs that mediate recognition of substrates.

In this work we also investigated the function of the Ptc2 noncatalytic domain. Since there is strong sequence similarity between the C-terminal residues of *S. cerevisiae* Ptc1 and sequences in Ptc2 and Ptc3 just prior to their noncatalytic domains, D-N-[VM]-[TS]-[VI]-X-[VI]-V-[FA]-L, we predicted that complete deletion of the Ptc2 noncatalytic domain would produce an active protein. However, neither Ptc2 (1-292) nor Ptc3 (1-293) was expressed in yeast (C. Young and I. Ota, unpublished data). Therefore, other Ptc2 truncation proteins were produced. Ptc2 (1-312) was expressed in yeast similarly to

the wild type, but it could not suppress *sln1Δ* lethality. We showed that this was due to its decreased catalytic activity relative to that of the full-length Ptc2 (Fig. 4C). Thus, unexpectedly, a portion of the Ptc2 noncatalytic domain is required for full catalytic activity.

We also noted that in some cases Ptc2 (1-355) and Ptc2 (1-412) suppressed *sln1Δ* lethality somewhat better than full-length Ptc2 (1-464). For example, the colonies of Ptc2 (1-355)- and Ptc2 (1-412)-bearing strains were often slightly larger than wild-type colonies on solid media containing 5-FOA. However, when these truncated proteins were expressed in *E. coli* and purified as His₆ fusion proteins, no obvious difference in their kinetic properties relative to those of the full-length Ptc2 could be detected (Fig. 4C). Interestingly, when expressed as HA epitope-tagged proteins in yeast, isolated by immunoprecipitation, and assayed with *pNPP*, Ptc2 (1-355) and Ptc2 (1-412) had slightly greater activity than the full-length Ptc2, although their expression levels were similar (C. Young and I. Ota, unpublished data). These data suggest that Ptc2 activity may be modified in yeast.

The subcellular localizations of Ptc2 and Ptc3 were also examined, and, like those of Ptc1, they were found to be cytoplasmic and nuclear (Fig. 5). Since Ptc2 and Ptc3 are ~50 kDa, close to the nuclear exclusion limit, ~40 to 60 kDa (4), and since the Ptc2-GFP and Ptc3-GFP fusions are beyond that limit, nuclear localization signals are likely present in these phosphatases. Thus, the PTCs are unlike the two PTPs that act on Hog1, which show differences in localization; Ptp2 is nuclear and appears excluded from the cytoplasm, whereas Ptp3 is cytoplasmic and is nonnuclear (19). However, like the PTPs, the PTCs showed no change in subcellular localization in response to signal. As far as we are aware, none of the protein phosphatases that inactivate MAPKs in yeast or vertebrates change localization in response to signal. Therefore, the activity of Hog1 and other MAPKs, which translocate from the cytoplasm to the nucleus upon activation (5, 18, 31), is regulated by protein phosphatases whose localization is static.

Comparison of the three PTCs in the HOG pathway shows they have complementary functions (summarized in Fig. 6). Previously, we showed that Ptc1 regulates the basal level of Hog1 phosphorylation and is required for dephosphorylation of Hog1 during adaptation (Fig. 6A) (37). Deletion of *PTC1* resulted in basal Hog1 activity sixfold greater than that for the wild type. As shown in Fig. 6A, in the absence of stress, Hog1 activity in the *ptc1Δ* strain was already 20% of the stress-induced activity in the wild type. In addition, the *ptc1Δ* strain failed to inactivate Hog1 during adaptation (Fig. 6A). The *ptc1Δ* strain also showed a defect in its ability to activate Hog1, and this may be due to increased levels of negative regulators. For example, *PTP2* and *PTP3* transcripts are known to be upregulated when Hog1 is activated (12). In contrast, the *ptc2Δ ptc3Δ* strain did not show a strong change in basal Hog1 activity or in adaptation. Instead, it showed higher Hog1 activation in response to stress (Fig. 3B and 6B).

The phenotypic effect of deleting PTCs was consistent with their roles in this pathway as defined by analysis of Hog1 activity. For example, deletion of *PTC1* resulted in a phenotype consistent with regulation of basal Hog1 activity. The *ptc1Δ ptp2Δ* mutant exhibits a strong growth defect under standard growth conditions at 30°C (14), which is due to *HOG1* (12).

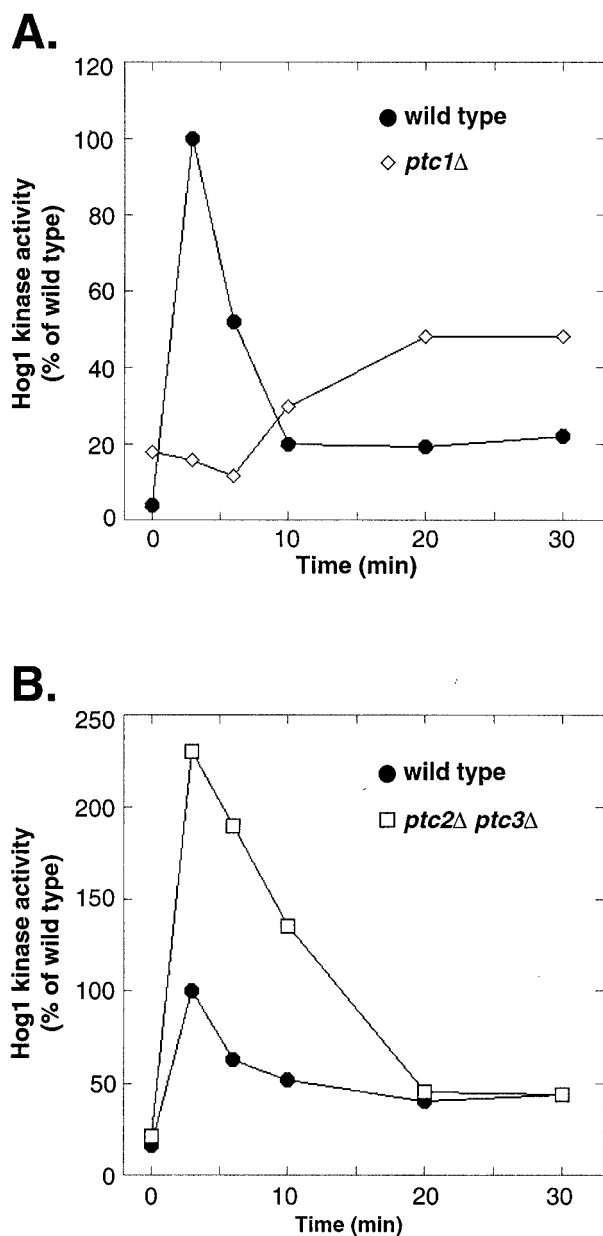


FIG. 6. Ptc1 regulation of Hog1 differs from Ptc2 and Ptc3. (A) Deletion of *PTC1* results in high basal Hog1 activity and an inability to inactivate Hog1 during adaptation. In addition, Hog1 showed a delay in activation and could not be fully activated in the *ptc1Δ* strain. The percentages of Hog1 activity relative to its maximal activity in the wild type are shown. Data are taken from Warmka et al. (37). (B) Deletion of *PTC2* and *PTC3* allowed Hog1 to be activated to a higher maximal activity than that for the wild type. No significant effects on basal activity or inactivation of Hog1 during adaptation were seen. Data are taken from Fig. 3B, and the percentages of Hog1 activity relative to that for the wild type at its maximum are shown.

This result suggests that Hog1 is hyperphosphorylated in the *ptc1Δ ptp2Δ* mutant in the absence of stress. Indeed, Hog1 activity was increased in the *ptc1Δ* mutant prior to stress (37), as was the level of Hog1-pY in the *ptp2Δ* mutant (12, 40). In contrast, deletion of *PTC2* and/or *PTC3* together with *PTP2* produced no obvious defect under standard growth conditions

(Fig. 1), consistent with the result that deletion of *PTC2* and *PTC3* had little effect on basal Hog1 kinase activity (Fig. 3B).

Other phenotypic data supported the idea that Ptc2 and Ptc3 regulate maximal Hog1 activity. We recently showed that Hog1 is activated by heat stress and that deletion of *PTP2* and *PTP3*, which encode PTPs that inactivate Hog1, is lethal at 37°C due to Hog1 hyperactivation (38). In this work we showed that deletion of *PTCs* together with *PTP2* produced a temperature-sensitive defect dependent on *HOG1*. For example, the *ptc3Δ ptp2Δ* (Fig. 1A), *ptc2Δ ptp2Δ* (data not shown), and *ptc2Δ ptc3Δ ptp2Δ* (Fig. 1A) strains grew poorly at 37°C, and deletion of *HOG1* suppressed these defects (Fig. 1B). These results suggest that the growth defect of the *ptcΔ ptp2Δ* strains at high temperature is due to increased maximal activity of Hog1. An additional phenotype was that the *ptc2Δ ptc3Δ* and *ptc2Δ ptc3Δ ptp2Δ* strains showed some enhanced ability to grow on solid media containing 0.9 to 1.4 M NaCl (J. Mapes and I. Ota, unpublished data). This phenotype is also consistent with stress inducing higher Hog1 activity in the phosphatase-null strains. One point that remains unclear is why heat stress is lethal to phosphatase-null strains, while osmotic stress is not. The simplest explanation is that heat stress induces physiological changes different from those induced by osmotic stress, which, when combined with Hog1 hyperactivation, are lethal. For example, as the cell wall integrity MAPK pathway is activated by heat stress and as the PTPs also inactivate this pathway, lethality may be due to misregulation of both this and the HOG pathways.

Ptc1 also differed from Ptc2 and -3 in its effects on adaptation. Previously, we showed that Ptc1 was required for adaptation, as Hog1 is poorly inactivated in the *ptc1Δ* mutant compared to its inactivation in the wild type (Fig. 6A) (37). For example, the *ptc1Δ* strain retained high Hog1 activity even after 1 h of osmotic stress (37). However, the *ptc2Δ ptc3Δ* strain showed no defect in adaptation (Fig. 3B and 6B). How Ptc2 and Ptc3 affect Hog1 maximal activity but not Hog1 inactivation during adaptation is not known. One possibility is that Ptc2 and Ptc3 activity is differentially regulated during Hog1 activation and adaptation. This hypothesis will require further investigation.

ACKNOWLEDGMENTS

We thank Ji Lee for constructing the pKT-PTC2 plasmid and Chris Arkind and Anne Burkholder for constructing the *ptc2Δ ptc3Δ ptp2Δ* and *ptc2Δ ptp2Δ hog1Δ* yeast strains, respectively. We thank Chris Mattison and Amanda Reynolds for helpful comments and critical reading of the manuscript.

This work was supported by a grant from the American Cancer Society.

REFERENCES

- Barford, D. 1996. Molecular mechanisms of the protein serine/threonine phosphatases. *Trends Biochem. Sci.* **21**:407–412.
- Bartel, B., I. Wunning, and A. Varshavsky. 1990. The recognition component of the N-end rule pathway. *EMBO J.* **9**:3179–3189.
- Brachmann, C. B., A. Davies, G. J. Cost, E. Caputo, J. Li, P. Hieter, and J. D. Boeke. 1998. Designer deletion strains derived from *Saccharomyces cerevisiae* S288C: a useful set of strains and plasmids for PCR-mediated gene disruption and other applications. *Yeast* **14**:115–132.
- Davis, L. I. 1995. The nuclear pore complex. *Annu. Rev. Biochem.* **64**:865–896.
- Ferrigno, P., F. Posas, D. Koepp, H. Saito, and P. A. Silver. 1998. Regulated nucleo/cytoplasmic exchange of HOG1 MAPK requires the importin beta homologs NMD5 and XPO1. *EMBO J.* **17**:5606–5614.

6. Gaits, F., K. Shiozaki, and P. Russell. 1997. Protein phosphatase 2C acts independently of stress-activated kinase cascade to regulate the stress response in fission yeast. *J. Biol. Chem.* **272**:17873–17879.
7. Gietz, R. D., and A. Sugino. 1988. New yeast-*Escherichia coli* shuttle vectors constructed with in vitro mutagenized yeast genes lacking six-base pair restriction sites. *Gene* **74**:527–534.
8. Gustin, M. C., J. Albertyn, M. Alexander, and K. Davenport. 1998. MAP kinase pathways in the yeast *Saccharomyces cerevisiae*. *Microbiol. Mol. Biol. Rev.* **62**:1264–1300.
9. Hanada, M., T. Kobayashi, M. Ohnishi, S. Ikeda, H. Wang, K. Katsura, Y. Yanagawa, A. Hiraga, R. Kanamaru, and S. Tamura. 1998. Selective suppression of stress-activated protein kinase pathway by protein phosphatase 2C in mammalian cells. *FEBS Lett.* **437**:172–176.
10. Hanada, M., J. Ninomiya-Tsuji, K. Komaki, M. Ohnishi, K. Katsura, R. Kanamaru, K. Matsumoto, and S. Tamura. 2001. Regulation of the TAK1 signaling pathway by protein phosphatase 2C. *J. Biol. Chem.* **276**:5753–5759.
11. Hovland, P., J. Flick, M. Johnston, and R. A. Sclafani. 1989. Galactose as a gratuitous inducer of GAL gene expression in yeasts growing on glucose. *Gene* **83**:57–64.
12. Jacoby, T., H. Flanagan, A. Faykin, A. G. Seto, C. Mattison, and I. Ota. 1997. Two protein-tyrosine phosphatases inactivate the osmotic stress response pathway in yeast by targeting the mitogen-activated protein kinase, Hog1. *J. Biol. Chem.* **272**:17749–17755.
13. Maeda, T., M. Takekawa, and H. Saito. 1995. Activation of yeast PBS2 MAPKK by MAPKKs or by binding of an SH3-containing osmosensor. *Science* **269**:554–558.
14. Maeda, T., A. Y. Tsai, and H. Saito. 1993. Mutations in a protein tyrosine phosphatase gene (*PTP2*) and a protein serine/threonine phosphatase gene (*PTCI*) cause a synthetic growth defect in *Saccharomyces cerevisiae*. *Mol. Cell. Biol.* **13**:5408–5417.
15. Maeda, T., S. M. Wurgler-Murphy, and H. Saito. 1994. A two-component system that regulates an osmosensing MAP kinase cascade in yeast. *Nature* **369**:242–245.
16. Mann, D. J., D. G. Campbell, C. H. McGowan, and P. T. Cohen. 1992. Mammalian protein serine/threonine phosphatase 2C: cDNA cloning and comparative analysis of amino acid sequences. *Biochim. Biophys. Acta* **1130**:100–104.
17. Martin-Blanco, E., A. Gampel, J. Ring, K. Virdee, N. Kirov, A. M. Tolkovsky, and A. Martinez-Arias. 1998. *puckered* encodes a phosphatase that mediates a feedback loop regulating JNK activity during dorsal closure in *Drosophila*. *Genes Dev.* **12**:557–570.
18. Mattison, C. P., and I. M. Ota. 2000. Two protein tyrosine phosphatases, Ptp2 and Ptp3, modulate the subcellular localization of the Hog1 MAP kinase in yeast. *Genes Dev.* **14**:1229–1235.
19. Mattison, C. P., S. S. Spencer, K. A. Kresge, J. Lee, and I. M. Ota. 1999. Differential regulation of the cell wall integrity mitogen-activated protein kinase pathway in budding yeast by the protein tyrosine phosphatases Ptp2 and Ptp3. *Mol. Cell. Biol.* **19**:7651–7660.
20. Meskiene, I., L. Bogre, W. Glaser, J. Balog, M. Brandstotter, K. Zwerger, G. Ammerer, and H. Hirt. 1998. MP2C, a plant protein phosphatase 2C, functions as a negative regulator of mitogen-activated protein kinase pathways in yeast and plants. *Proc. Natl. Acad. Sci. USA* **95**:1938–1943.
21. Mitchell, D. A., T. K. Marshall, and R. J. Deschenes. 1993. Vectors for the inducible overexpression of glutathione S-transferase fusion proteins in yeast. *Yeast* **9**:715–722.
22. Nguyen, A. N., and K. Shiozaki. 1999. Heat-shock-induced activation of stress MAP kinase is regulated by threonine- and tyrosine-specific phosphatases. *Genes Dev.* **13**:1653–1663.
23. O'Rourke, S. M., and I. Herskowitz. 1998. The Hog1 MAPK prevents cross talk between the HOG and pheromone response MAPK pathways in *Saccharomyces cerevisiae*. *Genes Dev.* **12**:2874–2886.
24. Ota, I. M., and A. Varshavsky. 1993. A yeast protein similar to bacterial two-component regulators. *Science* **262**:566–569.
25. Pearson, G., F. Robinson, T. B. Gibson, B. E. Xu, M. Karandikar, K. Berman, and M. H. Cobb. 2001. Mitogen-activated protein (MAP) kinase pathways: regulation and physiological functions. *Endocr. Rev.* **22**:153–183.
26. Posas, F., and H. Saito. 1997. Osmotic activation of the HOG MAPK pathway via Ste11p MAPKKK: scaffold role of Pbs2p MAPKK. *Science* **276**:1702–1705.
27. Posas, F., E. A. Witten, and H. Saito. 1998. Requirement of STE50 for osmotic stress-induced activation of the STE11 mitogen-activated protein kinase kinase in the high-osmolarity glycerol response pathway. *Mol. Cell. Biol.* **18**:5788–5796.
28. Posas, F., S. M. Wurgler-Murphy, T. Maeda, E. A. Witten, T. C. Thai, and H. Saito. 1996. Yeast HOG1 MAP kinase cascade is regulated by a multistep phosphorelay mechanism in the SLN1-YPD1-SSK1 “two-component” osmosensor. *Cell* **86**:865–875.
29. Raitt, D. C., F. Posas, and H. Saito. 2000. Yeast Cdc42 GTPase and Ste20 PAK-like kinase regulate Sho1-dependent activation of the Hog1 MAPK pathway. *EMBO J.* **19**:4623–4631.
30. Ramezani Rad, M., G. Jansen, F. Buhning, and C. P. Hollenberg. 1998. Ste50p is involved in regulating filamentous growth in the yeast *Saccharomyces cerevisiae* and associates with Ste11p. *Mol. Gen. Genet.* **259**:29–38.
31. Reiser, V., H. Ruis, and G. Ammerer. 1999. Kinase activity-dependent nuclear export opposes stress-induced nuclear accumulation and retention of Hog1 mitogen-activated protein kinase in the budding yeast *Saccharomyces cerevisiae*. *Mol. Biol. Cell* **10**:1147–1161.
32. Robinson, M. K., W. H. van Zyl, E. M. Phizicky, and J. R. Broach. 1994. *TPD1* of *Saccharomyces cerevisiae* encodes a protein phosphatase 2C-like activity implicated in tRNA splicing and cell separation. *Mol. Cell. Biol.* **14**:3634–3645.
33. Sherman, F., G. R. Fink, and J. B. Hicks. 1986. *Methods in yeast genetics*. Cold Spring Harbor Laboratory, Cold Spring Harbor, N.Y.
34. Sikorski, R. S., and P. Hieter. 1989. A system of shuttle vectors and yeast host strains designed for efficient manipulation of DNA in *Saccharomyces cerevisiae*. *Genetics* **122**:19–27.
35. Takekawa, M., T. Maeda, and H. Saito. 1998. Protein phosphatase 2C α inhibits the human stress-responsive p38 and JNK MAPK pathways. *EMBO J.* **17**:4744–4752.
36. Walter, G., and M. Mumby. 1993. Protein serine/threonine phosphatases and cell transformation. *Biochim. Biophys. Acta* **1155**:207–226.
37. Warmka, J., J. Hanneman, J. Lee, D. Amin, and I. Ota. 2001. Ptc1, a type 2C Ser/Thr phosphatase, inactivates the HOG pathway by dephosphorylating the mitogen-activated protein kinase Hog1. *Mol. Cell. Biol.* **21**:51–60.
38. Winkler, A., C. Arkind, C. P. Mattison, A. Burkholder, K. Knoche, and I. Ota. 2002. Heat stress activates the yeast high-osmolarity glycerol mitogen-activated protein kinase pathway, and protein tyrosine phosphatases are essential under heat stress. **1**:163–173.
39. Wolfe, K. H., and D. C. Shields. 1997. Molecular evidence for an ancient duplication of the entire yeast genome. *Nature* **387**:708–713.
40. Wurgler-Murphy, S. M., T. Maeda, E. A. Witten, and H. Saito. 1997. Regulation of the *Saccharomyces cerevisiae* HOG1 mitogen-activated protein kinase by the PTP2 and PTP3 protein tyrosine phosphatases. *Mol. Cell. Biol.* **17**:1289–1297.
41. Zeitlinger, J., and D. Bohmann. 1999. Thorax closure in *Drosophila*: involvement of Fos and the JNK pathway. *Development* **126**:3947–3956.